Available online at www.sciencedirect.com
SCIENCE DIRECT®
Coordination Chemistry Reviews 249 (2005) 1396–1409
COORDINATION CHEMISTRY REVIEWS
www.elsevier.com/locate/ccr

Review

Electronic spectroscopy and photophysics of metal–alkylidyne complexes

Ryan E. Da Re[a,b], Michael D. Hopkins[a,*]

[a] *Department of Chemistry, The University of Chicago, 5735 S. Ellis Avenue, Chicago, IL 60637, USA*
[b] *Structural and Isotope Chemistry Group, Chemistry Division, MS J514, Los Alamos National Laboratory, Los Alamos, NM 87545, USA*

Received 4 November 2004; accepted 10 March 2005
Available online 4 May 2005

Dedicated to the memory of our friend Vinny Miskowski.

Contents

1. Introduction 1396
2. Electronic structures and spectra 1397
   2.1. Molecular orbitals 1397
   2.2. Comparisons to metal–oxo complexes 1398
   2.3. Electronic transitions and states 1399
      2.3.1. $\pi \rightarrow \pi^*$ Transitions and states 1399
      2.3.2. $d_{xy} \rightarrow \pi^*$ and $\pi \rightarrow d_{xy}$ transitions and states 1402
3. Photophysical properties of d^2 complexes 1404
   3.1. Emissive $d_{xy} \rightarrow \pi^*$ excited states 1404
   3.2. Emissive $\pi \rightarrow \pi^*$ excited states 1406
   3.3. MLCT excited states 1407
4. Photophysical properties of d^1 complexes 1407
5. Photophysical properties of d^0 complexes 1408
6. Concluding remarks 1408
   Acknowledgments 1409
   References 1409

Abstract

The electronic-absorption and -emission spectroscopy and photophysical properties of metal–alkylidyne (–carbyne) complexes are reviewed. Emission has been observed in fluid solution at room temperature from compounds of a variety of different metals (Mo, W, Re, Os) and electron configurations (d^0, d^1, d^2). The emissive excited states are of the types $d_{xy} \rightarrow \pi^*$, $\pi \rightarrow \pi^*$, $\pi \rightarrow d_{xy}$, and MLCT. This compositional and electronic diversity enables the luminescence properties of metal–alkylidyne complexes to be broadly tuned.

Keywords: Excited state; Luminescence; Emission lifetime; Quantum yield; Spin–orbit coupling

1. Introduction

Nearly 20 years ago, Bocarsly et al. reported the first examples of metal–alkylidyne (–carbyne) complexes that luminesce in fluid solution at room temperature [1]. Since then, the

* Corresponding author. Tel.: +1 773 702 6490; fax: +1 773 702 0805.
E-mail address: mhopkins@uchicago.edu (M.D. Hopkins).

0010-8545/$ – see front matter © 2005 Elsevier B.V. All rights reserved.
doi:10.1016/j.ccr.2005.03.011

class of luminescent metal–alkylidyne complexes has grown to nearly 50 members [2–16]. Although this class of complexes is still relatively small in size, it is remarkably diverse: it includes derivatives of several different metals (Mo, W, Re, Os), with three different d-electron configurations (d^0, d^1, d^2), and bearing ancillary ligands that span the spectrochemical series (e.g., CO, PR_3, H_2O, and OR). Moreover, emissive excited states with four different orbital configurations and spin-multiplicities have been identified.

The fact that emissive metal–alkylidyne complexes exhibit such a wide range of electronic characteristics suggests that their excited-state properties might be especially broadly tunable. This is of interest both from a fundamental standpoint and in terms of the design of new types of photoredox catalysts and electronic materials, particularly π-conjugated systems in which [$L_nM{\equiv}C$] fragments are used as electronically tunable, function-rich (photo- and redox-active) replacements for C≡C bonds. Several preliminary studies along these latter lines suggest that this is a promising area of development.

The aim of this review is to discuss the electronic-spectroscopic and photophysical data for emissive metal–alkylidyne complexes in the context of a basic theoretical description of their orbitals and electronic states. The ground-state chemistry and properties of metal–alkylidyne complexes have been the subject of regular reviews [17,18].

2. Electronic structures and spectra

2.1. Molecular orbitals

Luminescent metal–alkylidyne complexes share a number of structural and electronic features, which allows their spectroscopic and photophysical properties to be considered within a common theoretical framework. Specifically, all derivatives reported to date possess pseudo-octahedral (or pseudo-tetragonal) structures; their emissive excited states, with one minor exception, are largely or exclusively derived from orbitals localized within the M≡C–R moiety; and the alkylidyne R group is phenyl or a substituted aryl group. Thus, the relevant molecular orbitals and electronic states for this discussion are those of a C_{2v} symmetry M(CPh)L_5 complex. These are most easily thought of in terms of their relationship to the orbitals and states of an idealized C_{4v} symmetry M(CH)L_5 complex.

The molecular orbital diagram of a M(CH)L_5 complex is shown in Fig. 1. This picture is qualitatively similar to that developed many years ago for analogous ML_5 (and NL_5) complexes, which have been discussed in detail elsewhere [19]. The M≡C σ-bonding and σ-antibonding molecular orbitals (1a_1[σ(MC)] and 2a_1[σ^*(MC)]) are formed from combinations of the ML_5 d_{z^2} and CH sp_z (σ) orbitals, and the M≡C π-bonding (1e[π(MC)]) and π-antibonding (2e[π^*(MC)]) molecular orbitals are formed from combinations of the ML_5 d_{xz},d_{yz} orbitals and CH p_x,p_y orbitals. By analogy to

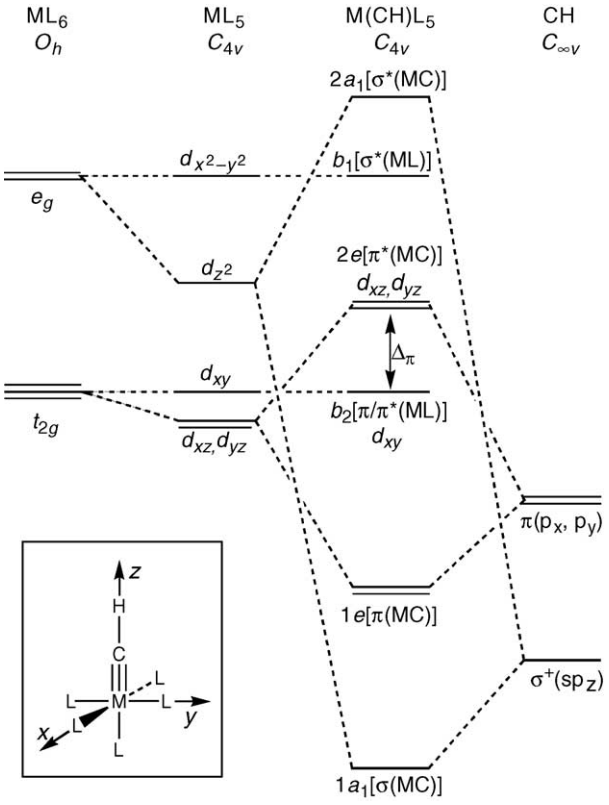

Fig. 1. Molecular orbital diagram for M(CH)L_5. The coordinate system is shown in the inset.

metal–oxo and –nitrido complexes the π^*(MC) orbitals are labeled as being principally of d orbital parentage, although this is an oversimplification (vide infra). Mid gap between M≡C π and π^* orbitals lies the d_{xy} orbital (b_2), which is nonbonding with respect to the CH ligand and, thus, unchanged in energy relative to the ML_5 fragment (to a first approximation). The d_{xz} and d_{yz} orbitals are destabilized relative to the d_{xy} orbital by an energy denoted Δπ. For second- and third-transition-series metal–alkylidyne complexes, Δπ is anticipated to be of similar magnitude to that for mono-oxo and -nitrido metal complexes (>20,000 cm^{-1} [19]), due to strong M–C π-bonding. A formal metal–carbon bond order of three is maintained with electronic configurations of $[\sigma(MC)]^2[\pi(MC)]^4$ ($^1A_1$), $[\sigma(MC)]^2[\pi(MC)]^4[d_{xy}]^1$ ($^2B_2$), and $[\sigma(MC)]^2[\pi(MC)]^4[d_{xy}]^2$ ($^1A_1$). These correspond to formal d-electron counts of d^0, d^1, and d^2, respectively, if the alkylidyne ligand is counted as a trianion, i.e., the d_{xz},d_{yz} orbitals are "assigned" to the π^*(MC) orbital (vide infra).

All luminescent metal–alkylidyne complexes reported to date bear a phenyl (or aryl) alkylidyne R group, rather than the cylindrically symmetric R group (e.g., R = H) for which Fig. 1 is appropriate. This substitution reduces the molecular symmetry from C_{4v} to C_{2v} and lifts the degeneracies of the π(MC) and π^*(MC) orbitals. The molecular orbital diagram for M(CPh)L_5 complexes is shown in Fig. 2. The π-conjugation between the phenyl and M≡C moieties destabilizes the π(MC) orbital perpendicular to the phenyl plane

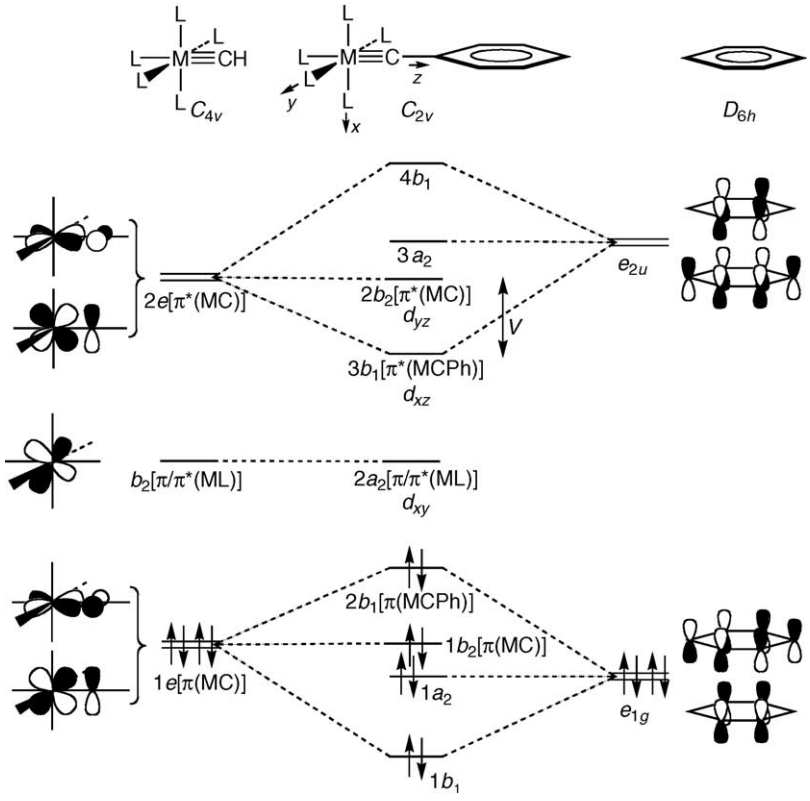

Fig. 2. Molecular orbital diagram for M(CPh)L_5. A ground-state d^0 electronic configuration is shown. For d^1 and d^2 configurations, the d_{xy} orbital ($2a_2$) is occupied by one and two electrons, respectively.

($2b_1$, which is C–Ph π-antibonding) relative to the π(MC) orbital parallel to the phenyl plane ($1b_2$), and stabilizes the out-of-plane π^*(MC) orbital ($3b_1$, which is C–Ph π-bonding) relative to the in-plane π^*(MC) orbital ($2b_2$). The orbital splitting arising from MC–Ph π conjugation is denoted *V*. The loss of π orbital degeneracy does not affect the relationship between metal–carbon bond order and d-electron count; formal metal–carbon triple bonds are maintained with d^0, d^1, and d^2 electronic configurations. The ground-state configurations and symmetries for d^0, d^1, and d^2 M(CPh)L_5 complexes are set out in Table 1.

Deeper insights into the nature of the metal–carbon triple bond may be gleaned, of course, from theoretical calculations [20]. However, the symmetry-based arguments provided here are sufficient to interpret the spectroscopic and photophysical data for metal–alkylidyne complexes.

Table 1
Electronic transitions and states of C_{2v} symmetry M(CPh)L_5 complexes[a]

d^n	Ground state	Orbital transition	Excited states
d^2	$[\pi(MCPh)]^2[d_{xy}]^2$, $^1A_1$	$d_{xy} \rightarrow \pi^*$ ($2a_2 \rightarrow 3b_1$)	$^1B_2$, $^3B_2$
		$\pi \rightarrow \pi^*$ ($2b_1 \rightarrow 3b_1$)	$^1A_1$, $^3A_1$
d^1	$[\pi(MCPh)]^2[d_{xy}]^1$, $^2A_2$	$d_{xy} \rightarrow \pi^*$ ($2a_2 \rightarrow 3b_1$)	$^2B_1$
		$\pi \rightarrow d_{xy}$ ($2b_1 \rightarrow 2a_2$)	$^2B_1$
		$\pi \rightarrow \pi^*$ ($2b_1 \rightarrow 3b_1$)	$^2A_2$, $^4A_2$
d^0	$[\pi(MCPh)]^2$, $^1A_1$	$\pi \rightarrow d_{xy}$ ($2b_1 \rightarrow 2a_2$)	$^1B_2$, $^3B_2$
		$\pi \rightarrow \pi^*$ ($2b_1 \rightarrow 3b_1$)	$^1A_1$, $^3A_1$

[a] See Fig. 2.

2.2. Comparisons to metal–oxo complexes

It is intuitively reasonable to draw electronic analogies between metal–alkylidyne and metal–oxo (and –nitrido) complexes, such as those noted above, in view of the fact that there are isostructural families of complexes involving these triply bonded ligands; examples include the pairs of complexes W(CH)$(PMe_3)_4Cl$ and $[W(O)(PMe_3)_4Cl]^+$, and W(CR)$(OBu^t)_3$ and W(N)$(OBu^t)_3$. However, there are electronic differences between these multiply bonded ligands that have implications for the qualitative description of their orbitals and states.

One electronic difference between metal–alkylidyne and metal–oxo complexes is that CR valence orbitals are considerably higher in energy than are those of oxygen – the 2p valence orbital ionization energies of the elements differ by ca. 5 eV – and, so, lie closer to the t_{2g}-parentage orbitals of a given ML_5 fragment than do the p orbitals of oxygen. While it is reasonable to designate π^*(MO) orbitals as being mainly of d_{xz},d_{yz} parentage [19], this description is not generally valid for the π^*(MC) orbitals; they may be largely carbon or CR in character. (Similarly, π(MC) orbitals possess more d orbital character than do π(MO) orbitals.) The fact that the metal and CR orbitals are close in energy has led to the use of two different electron-counting formalisms for the CR ligand in the literature. At one limit are complexes bearing multiple anionic ancillary ligands, of

which Schrock's $M(CR)X_3$ complexes (M = Mo, W; X = R, OR, SR, NR_2) are the archetypal examples. For these compounds, the alkylidyne ligand is counted as CR^{3-}, by analogy to the nitrido ligand. At the other limit are the classic Fischer complexes of the form $M(CR)(CO)_4X$ (M = Cr, Mo, W; X = halide) and other compounds with π-acceptor ligands, for which the alkylidyne ligand is typically counted as CR^+. On the basis of these descriptions, the alkylidyne ligand has been described, in different publications, as being a stronger π-donor than the nitrido ligand and a stronger π-acceptor than carbon monoxide! Fortunately, these semantic distinctions (which simply describe the limits $E[ML_5(t_{2g})] > E[C(p_x,p_y)]$ and $E[ML_5(t_{2g})] < E[C(p_x,p_y)]$) are of no consequence with regard to the assignment of the electronic spectra and emissive states of the compounds because the orbital symmetries do not depend on the orbital parentage. For consistency with the spectroscopic literature for metal–oxo and –nitrido complexes, we will refer throughout to d^0, d^1, or d^2 electron counts (i.e., the CR^{3-} convention), without regard to whether these designations are strictly appropriate for the specific complex in question. These d^n configurations become d^{n+4} if one switches from the CR^{3-} to CR^+ convention.

A second electronic difference between metal–alkylidyne and metal–oxo complexes is that the former can support multiple π-acceptor ancillary ligands (e.g., $M(CR)(CO)_4X$), whereas this is uncommon for metal–oxo compounds. The convention in the spectroscopic and photophysical literature for MOL_5 and MNL_5 compounds is to denote the d_{xy} orbital (b_2, Fig. 1; $2a_2$, Fig. 2) as "nonbonding"; electronic transitions of metal–oxo and –nitrido complexes involving this orbital are denoted, for example, "$n \rightarrow \pi^*$" [19]. The nonbonding designation is only strictly correct with respect to the oxo and *trans* L ligands, not the equatorial ligands, but it is a reasonable approximation in the latter case because the d_{xy} orbital energy is not strongly sensitive to the nature of the equatorial ligands typically found for these compounds. For metal–alkylidyne complexes with ancillary carbonyl ligands, however, the "nonbonding" description is clearly vitiated due to strong d_{xy}–π^*(CO) interactions. The d_{xy} orbital is labeled [π/π*(ML)] in Figs. 1 and 2 to reflect this fact, and the nonbonding "n" designation is not used here even though it may be applicable in specific cases.

2.3. Electronic transitions and states

The electronic transitions of $M(CPh)L_5$ complexes that involve exclusively the frontier $2b_1[\pi(MCPh)]$, $3b_1[\pi^*(MCPh)]$, and $2a_2[d_{xy}]$ orbitals (Fig. 2) are the $\pi \rightarrow \pi^*$ transition, which will be observed for d^0, d^1, and d^2 complexes; the $\pi \rightarrow d_{xy}$ transition, for d^0 and d^1 complexes; and the $d_{xy} \rightarrow \pi^*$ transition, for d^1 and d^2 complexes. The symmetries of the excited states produced by these transitions are set out in Table 1. There have been no polarized single-crystal spectroscopic studies to definitively assign the electronic spectra of metal–alkylidyne complexes. Instead, assignments typically have been made on the basis of band shifts upon ligand substitution, quantum–chemical calculations, and/or comparisons to analogous, well studied metal–oxo and –nitrido complexes. In this section, a few general points about these transitions and excited states are made with reference to experimental data for $M(CPh)L_5$ (and, more broadly, $M(CAr)L_5$) complexes.

2.3.1. $\pi \rightarrow \pi^*$ Transitions and states

The electric-dipole-allowed $2b_1[\pi(MCAr)] \rightarrow 3b_1[\pi^*(MCAr)]$ transition (hereafter denoted $\pi \rightarrow \pi^*$) is common to d^0, d^1, and d^2 $M(CAr)L_5$ complexes. For nearly all luminescent complexes, a strong (ε, $10^4\,M^{-1}\,cm^{-1}$) band is observed in the electronic-absorption spectrum in the region 290–360 nm (Table 2); this band is typically assigned to the spin-allowed $\pi \rightarrow \pi^*$ transition ($^1A_1 \rightarrow {}^1A_1$ for d^0 and d^2, $^2A_2 \rightarrow {}^2A_2$ for d^1; Table 1). Although this region of the electronic spectrum is often congested with other bands arising from charge-transfer and intraligand transitions, the relatively modest sensitivity of the band position and intensity to the nature of the ancillary ligands on the metal, but stronger dependence on the donor–acceptor character of aryl substituents, are fully consistent with this assignment. Perhaps the simplest chromophore in this regard is the d^2 ion $[Os(CPh)(NH_3)_5]^{3+}$ [9]; it exhibits a strong band at 292 nm (ε, $14300\,M^{-1}\,cm^{-1}$) for which the only logical assignment is to $^1[\pi \rightarrow \pi^*]$. Theoretical support for the appearance of the $^1[\pi \rightarrow \pi^*]$ band in this region comes from a CI-singles calculation by Che and co-workers on the hypothetical d^2 ion $[Re(CPh)(H_2PCHCHPH_2)_2Cl]^+$; the band was predicted to lie at 290 nm, in reasonable agreement with the observed band for $[Re(CAr')(Ph_2PC_6H_4\text{-}2\text{-}PPh_2)_2Cl]^+$ (318 nm) [13]. The electronic-absorption spectrum of d^2 $W(CPh)(depe)_2Cl$ (depe: 1,2-bis(diethylphosphino)ethane), shown in Fig. 3, exhibits a representative $^1[\pi \rightarrow \pi^*]$ band at 336 nm [21]. The weak shoulder on the red flank, ca. 1300 cm^{-1} from the band

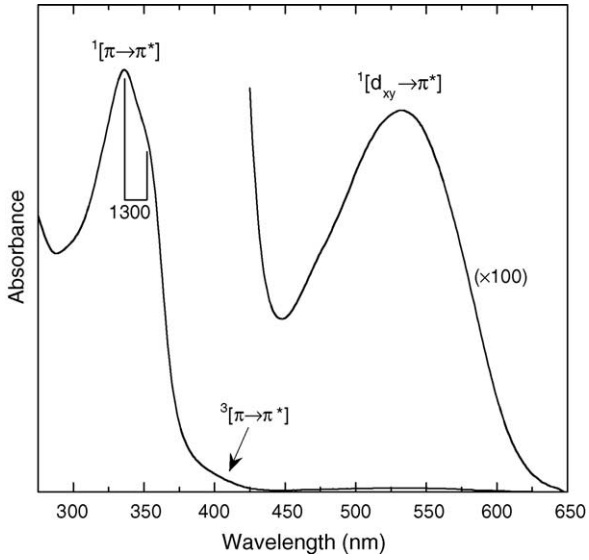

Fig. 3. Electronic-absorption spectrum of $W(CPh)(depe)_2Cl$ (2-methylpentane solution, 300 K).

Table 2
Electronic-spectroscopic and photophysical data for luminescent metal–alkylidyne complexes[a]

Compound	Absorption		Emission						Refs.
	λ_{max}, nm (ε, $M^{-1}\,cm^{-1}$)	Transition	λ_{max} (nm)	τ	ϕ	k_r ($10^3\,s^{-1}$)	k_{nr} ($10^6\,s^{-1}$)	Solvent	
d^2 Compounds									
$W(CPh)(CO)_2(tmeda)Cl$	448 (393) 330 (5500)	$^1[d_{xy} \rightarrow \pi^*]$ $^1[\pi \rightarrow \pi^*]$	640	285 ns	6.3×10^{-4}	2.2	3.5	Toluene	[1,2]
$W(CPh)(CO)_2(tmeda)Br$	450 (400) 327 (13000)	$^1[d_{xy} \rightarrow \pi^*]$ $^1[\pi \rightarrow \pi^*]$	630	180 ns	5.3×10^{-4}	2.9	5.6	Toluene	[1,2]
$W(CPh)(CO)_2(tmeda)I$	454 (560)	$^1[d_{xy} \rightarrow \pi^*]$	630	220 ns	1.5×10^{-4}	0.68	4.6	Toluene	[1,2]
$W(CPh)(CO)_2(py)_2Cl$	460sh (1064) 340 (17000)	$^1[d_{xy} \rightarrow \pi^*]$ $^1[\pi \rightarrow \pi^*]$	625	440 ns	7.8×10^{-4}	1.8	2.3	Toluene	[1,2]
$W(CPh)(CO)_2(py)_2Br$	460sh (1086) 350sh	$^1[d_{xy} \rightarrow \pi^*]$ $^1[\pi \rightarrow \pi^*]$	630					Toluene	[1,2]
$W(CPh)(CO)_2(dppe)Cl$	435 (368) 360 (10000)	$^1[d_{xy} \rightarrow \pi^*]$ $^1[\pi \rightarrow \pi^*]$	660[b]	232 ns	2.2×10^{-4}	0.95	4.3	Toluene	[1,2]
$W(C\text{-}2\text{-}C_{10}H_7)(CO)_2(py)_2Cl$	475 354	$^1[d_{xy} \rightarrow \pi^*]$ $^1[\pi \rightarrow \pi^*]$	660					Toluene	[1,2]
$W(CC_6H_4\text{-}4\text{-}NC)(CO)_2(tmeda)Cl$	476 (560)	$^1[d_{xy} \rightarrow \pi^*]$	656	0.5 μs	1.60×10^{-3}	3.2	2.0	CH_2Cl_2	[10]
$W(CC_6H_4\text{-}4\text{-}NC)(CO)_2(dppe)Cl$	456 (590)	$^1[d_{xy} \rightarrow \pi^*]$	664	0.2 μs				CH_2Cl_2	[10]
$W(CC_6H_4\text{-}4\text{-}NC)(CO)_2(dppe)Cl$	462 (950)	$^1[d_{xy} \rightarrow \pi^*]$	680	0.7 μs	1.14×10^{-3}	1.6	1.4	CH_2Cl_2	[10]
fac-$[W(CC_6H_4\text{-}4\text{-}NC)(CO)_2(tmeda)Cl]_2\text{-}ReCl(CO)_3$	490 (1640)	$^1[d_{xy} \rightarrow \pi^*]$	670	0.3 μs	1.98×10^{-3}	6.6	3.3	CH_2Cl_2	[10]
cis-$[W(CC_6H_4\text{-}4\text{-}NC)(CO)_2(tmeda)Cl]_2\text{-}PtI_2$	500 (1760)	$^1[d_{xy} \rightarrow \pi^*]$	682	0.2 μs	1.47×10^{-3}	7.4	5.0	CH_2Cl_2	[10]
fac-$[W(CC_6H_4\text{-}4\text{-}CCC_6H_4\text{-}4\text{-}NC)(CO)_2(dppe)Cl]_2ReCl(CO)_3$	464 (2980)	$^1[d_{xy} \rightarrow \pi^*]$	686	0.6 μs	9.4×10^{-4}	1.6	1.7	CH_2Cl_2	[10]
cis-$[W(CC_6H_4\text{-}4\text{-}CCC_6H_4\text{-}4\text{-}NC)(CO)_2(dppe)Cl]_2PdI_2$	470 (3050)	$^1[d_{xy} \rightarrow \pi^*]$	685	0.1 μs	1.9×10^{-4}	1.9	10.0	CH_2Cl_2	[10]
cis-$[W(CC_6H_4\text{-}4\text{-}CCC_6H_4\text{-}4\text{-}NC)(CO)_2(dppe)Cl]_2PtI_2$	470 (3130)	$^1[d_{xy} \rightarrow \pi^*]$	685	0.6 μs	9.0×10^{-4}	1.5	1.7	CH_2Cl_2	[10]
$W(CPh)(dppe)_2Cl$	525 sh 340	$^1[d_{xy} \rightarrow \pi^*]$ $^1[\pi \rightarrow \pi^*]$	675	303 ns	1.0×10^{-2}	33.0	3.3	Toluene	[11]
$CpW(CPh)(CO)\{P(OMe)_3\}$	483 (50) 329 (8000)	$^1[d_{xy} \rightarrow \pi^*]$ $^1[\pi \rightarrow \pi^*]$	747 741[c]	141 ns[c] 3.2 μs	6.9×10^{-4}	4.9	7.1	THF	[3,4]
$CpMo(CPh)(CO)\{P(OMe)_3\}$	477 (60) 328 (4000)	$^1[d_{xy} \rightarrow \pi^*]$ $^1[\pi \rightarrow \pi^*]$	787[c]	49 ns[d] 8.3 μs[c]	$<10^{-4}$	<2.0	20.4	THF	[3,4]
$CpW(C\text{-}o\text{-}Tol)(CO)\{P(OMe)_3\}$	476 331	$^1[d_{xy} \rightarrow \pi^*]$ $^1[\pi \rightarrow \pi^*]$	745 735[c]	170 ns 3.6 μs[c]	3.6×10^{-4}	2.1	5.9	THF	[3,4]
$CpW(C\text{-}2\text{-}Np)(CO)\{P(OMe)_3\}$	490 (70) 348 (6000)	$^1[d_{xy} \rightarrow \pi^*]$ $^1[\pi \rightarrow \pi^*]$	>780	66 ns				THF	[4]
$CpW(CPh)(CO)\{P(OPh)_3\}$	458 (200) 322 (9000)	$^1[d_{xy} \rightarrow \pi^*]$ $^1[\pi \rightarrow \pi^*]$	710	192 ns				MeCN	[5]
$[(Me_3TACN)W(CPh)(CO)_2]^+$	462 (240) 328 (7950)	$^1[d_{xy} \rightarrow \pi^*]$ $^1[\pi \rightarrow \pi^*]$	630	83 ns	1.6×10^{-4}	1.9	12.0	MeCN	[6]
$[(\eta^3\text{-}Ppy_3)W(CPh)(CO)_2]^+$	420 (5500) 342 (10200)	$^1[d_{xy} \rightarrow \pi^*]$ $^1[\pi \rightarrow \pi^*]$	633	250 ns	2.3×10^{-4}	0.92	4.0	CH_2Cl_2	[7]
$[(\eta^3\text{-}HCpy_3)W(CPh)(CO)_2]^+$	488 (890) 339 (12900)	$^1[d_{xy} \rightarrow \pi^*]$ $^1[\pi \rightarrow \pi^*]$	626	210 ns	3.3×10^{-4}	1.6	4.8	CH_2Cl_2	[7]
$[(\eta^3\text{-}Ppy_3)Mo(CPh)(CO)_2]^+$	496 (1820) 350 (4900)	$^1[d_{xy} \rightarrow \pi^*]$ $^1[\pi \rightarrow \pi^*]$	614	110 ns	2.0×10^{-4}	1.8	9.1	CH_2Cl_2	[7]
$[\{\eta^3\text{-}MeC(CH_2PPh_2)_3\}W(CPh)(CO)_2]^+$	488 (1480) 336 (7400)	$^1[d_{xy} \rightarrow \pi^*]$ $^1[\pi \rightarrow \pi^*]$	669	9 ns	1.1×10^{-4}	12.2	111	CH_2Cl_2	[7]
$[Os(CPh)(NH_3)_5]^{3+}$	462 (200) 292 (14300)	$^1[d_{xy} \rightarrow \pi^*]$ $^1[\pi \rightarrow \pi^*]$	632	55 ns	3.5×10^{-3}	63.4	18.1	MeCN	[9]
$[Os(CPh)(ND_3)_5]^{3+}$				62 ns	4.2×10^{-3}	67.8	16.1	MeCN	[9]

Table 2 (*Continued*)

Compound	Absorption		Emission						Refs.
	λ_{max}, nm (ε, $M^{-1}\,cm^{-1}$)	Transition	λ_{max} (nm)	τ	ϕ	k_r ($10^3\,s^{-1}$)	k_{nr} ($10^6\,s^{-1}$)	Solvent	
$[Re(CAr')(pdpp)_2Cl]^+$	410 (450) 318 (13900)	$^3[\pi \rightarrow \pi^*]$ $^1[\pi \rightarrow \pi^*]$	573	2.08 μs	4.2×10^{-2}	20.2	0.46	CH_2Cl_2	[12,13]
$[Re(CAr')(PPh_3)_2(CO)(H_2O)Cl]^+$	410 (1380)[b] 321 (13900)	$^3[\pi \rightarrow \pi^*]$ $^1[\pi \rightarrow \pi^*]$	580	2.25 μs	2.0×10^{-3}	0.89	0.44	CH_2Cl_2	[12,13]
$[Re(CAr')\{P(C_6H_4\text{-}4\text{-}OMe)_3\}_2(CO)(H_2O)Cl]^+$	420 (320)[b] 320 (13100)[b]	$^3[\pi \rightarrow \pi^*]$ $^1[\pi \rightarrow \pi^*]$	588	1.76 μs	6.7×10^{-3}	3.8	0.57	CH_2Cl_2	[12,13]
$[Re(CAr')(PMePh_2)_2(CO)(H_2O)Cl]^+$	410 (470)[b] 320 (12100)	$^3[\pi \rightarrow \pi^*]$ $^1[\pi \rightarrow \pi^*]$	611	0.95 μs	4.6×10^{-3}	4.8	1.1	CH_2Cl_2	[12,13]
$[Re(CAr')(dppe)(CO)_2Cl]^+$	430 (400)[b] 330 (7290)	$^3[\pi \rightarrow \pi^*]$ $^1[\pi \rightarrow \pi^*]$	567	3.35 μs	3.5×10^{-3}	1.1	0.30	CH_2Cl_2	[12,13]
$[Re(CAr')(Tp')(CO)_2]^+$	425 (970) 354 (15400)	$^3[\pi \rightarrow \pi^*]$ $^1[\pi \rightarrow \pi^*]$	585	1.48 μs	2.7×10^{-3}	1.8	0.67	CH_2Cl_2	[13]
$[Re(CC_6H_4\text{-}4\text{-}OMe)(pdpp)(CO)_2(OTf)]^+$	351 (25200)	$^1[\pi \rightarrow \pi^*]$	520	20 ns	1.5×10^{-4}	7.5	50.0	CH_2Cl_2	[13]
$[Re(CC_6H_4\text{-}4\text{-}Me)(pdpp)(CO)_2(OTf)]^+$	425 (300) 326 (18700)	$^3[\pi \rightarrow \pi^*]$ $^1[\pi \rightarrow \pi^*]$	527	220 ns	1.8×10^{-3}	8.2	4.5	CH_2Cl_2	[13]
$[Re(CPh)(pdpp)(CO)_2(OTf)]^+$	425 (380) 310 (14800)	$^3[\pi \rightarrow \pi^*]$ $^1[\pi \rightarrow \pi^*]$	530	530 ns	2.6×10^{-3}	4.9	1.9	CH_2Cl_2	[13]
$[Re(CC_6H_4\text{-}4\text{-}Cl)(pdpp)(CO)_2(OTf)]^+$	370 (1440) 325 (19200)	$^3[\pi \rightarrow \pi^*]$ $^1[\pi \rightarrow \pi^*]$	536	2.18 μs	1.2×10^{-2}	5.5	0.45	CH_2Cl_2	[13]
$[Re(CC_6H_4\text{-}4\text{-}Br)(pdpp)(CO)_2(OTf)]^+$	375 (3170) 329 (23200)	$^3[\pi \rightarrow \pi^*]$ $^1[\pi \rightarrow \pi^*]$	537	2.42 μs	1.1×10^{-2}	4.6	0.41	CH_2Cl_2	[13]
$[Re(CC_6H_4\text{-}4\text{-}CN)(pdpp)(CO)_2(OTf)]^+$	380 (860) 313 (18900)	$^3[\pi \rightarrow \pi^*]$ $^1[\pi \rightarrow \pi^*]$	559	4.84 μs	1.6×10^{-2}	3.3	0.20	CH_2Cl_2	[13]
$[Re(CAr')(bpy)(CO)_2Cl]^+$	340 (16400)	$d \rightarrow \pi^*(bpy)$	555	430 ns	2.5×10^{-4}	0.58	2.3	CH_2Cl_2	[13]
$[Re(CAr')(bpy\text{-}Cl_2)(CO)_2Cl]^+$	346 (15800)	$d \rightarrow \pi^*(bpy)$	575	70 ns	1.2×10^{-4}	1.7	14.3	CH_2Cl_2	[13]
$[Re(CAr')\{bpy\text{-}(CO_2Me)_2\}(CO)_2Cl]^+$	390 (9560)	$d \rightarrow \pi^*(bpy)$	580	610 ns	2.8×10^{-3}	4.6	1.6	CH_2Cl_2	[13]
d^1 Compounds									
$Re(CAr')(PPh_3)(H_2O)Cl_3$	658 (60) 550 (80)	$^2[d_{xy} \rightarrow \pi^*]$	696	490 ns	7×10^{-4}	1.4	2.0	CH_2Cl_2	[14]
$Re(CAr')(PPh_3)(H_2O)Br_3$	696 (90) 558 (180)	$^2[d_{xy} \rightarrow \pi^*]$	728	410 ns	6×10^{-3}	14.6	2.4	CH_2Cl_2	[14]
d^0 Compounds									
$[Na][W(CPh)(OBu^t)_4]$	~450sh	$^3[\pi \rightarrow \pi^*]$ or $^3[\pi^* \rightarrow d_{xy}]$	673	3.3 μs	2.1×10^{-4}	0.07	0.30	THF	[15]
	323	$^1[\pi \rightarrow \pi^*]$							
$[Na(15\text{-crown-}5)][W(CPh)(OBu^t)_4]$	~450sh	$^3[\pi \rightarrow \pi^*]$ or $^3[\pi^* \rightarrow d_{xy}]$	658	3.7 μs	1.4×10^{-4}	0.04	0.27	THF	[15]
	323	$^1[\pi \rightarrow \pi^*]$							
$[Na(crypt\text{-}2,2,2)][W(CPh)(OBu^t)_4]$	~450sh	$^3[\pi \rightarrow \pi^*]$ or $^3[\pi^* \rightarrow d_{xy}]$	676	2.8 μs	7×10^{-5}	0.03	0.36	THF	[15]
	332	$^1[\pi \rightarrow \pi^*]$							

[a] Measurements are at 300 K unless otherwise noted. In cases, where different values for a particular datum are reported in two different papers, the most recent value is listed. Ligand abbreviations: tmeda: *N*,*N*,*N*′,*N*′-tetramethylethylenediamine; dppe: 1,2-bis(diphenylphosphino)ethane; Np: naphthyl; Me_3TACN: 1,4,7-trimethyl-1,4,7-triazacyclononane; Ppy_3: tris(2-pyridyl)phosphine; $HCpy_3$: tris(2-pyridyl)methane; pdpp: *o*-phenylenebis(diphenylphosphine); Ar′: $C_6H_2Me_3$-2,4,6; Tp′: tris(3,5-dimethyl-1-pyrazolyl)borohydride; bpy-X_2: 4,4′-X-2,2′-bipyridine.

[b] Different value reported in the earlier paper.

[c] Measurement at 77 K.

[d] Lifetime measured by transient-kinetic spectroscopy.

maximum, is vibronic structure arising from a WCPh mode. (The vibrational spectra of metal–alkylidyne complexes have been discussed in detail elsewhere [22–24].)

It is interesting to compare the $^1[\pi \rightarrow \pi^*]$ transition energies of d^2 and d^0 $M(CPh)L_5$ complexes with that of phenylacetylene, which also possesses C_{2v} symmetry and, thus, π and π^* orbitals and $\pi \rightarrow \pi^*$ states that correspond to those of $M(CPh)L_5$. Phenylacetylene exhibits the analogous $^1[\pi \rightarrow \pi^*]$ band at ca. 235 nm [25], which is >1 eV higher in energy than for the metal–alkylidyne complexes. The red shift for $M(CPh)L_5$ complexes is a reflection of the strong contribution of the metal d_{xz},d_{yz} orbitals to the $2b_1[\pi(MCAr)]$ and $3b_1[\pi^*(MCAr)]$ orbitals; the corresponding orbitals of phenylacetylene, in contrast, have relatively little C≡C character [26].

An electronic-absorption band arising from the spin-forbidden $\pi \rightarrow \pi^*$ transition may also be observed for $M(CPh)L_5$ complexes ($^3[\pi \rightarrow \pi^*]$ for d^2 and d^0, $^4[\pi \rightarrow \pi^*]$ for d^1). Comparisons to second- and third-transition series oxo complexes suggest that this band should lie ca. 3000–5000 cm^{-1} to lower energy of the spin-allowed $\pi \rightarrow \pi^*$ band; it will also be substantially weaker in intensity. The electronic-absorption spectrum of $W(CPh)(depe)_2Cl$ (Fig. 3) exhibits a weak tail at the base of the $^1[\pi \rightarrow \pi^*]$ band, centered at ca. 395 nm, that is resolved into a distinct shoulder at 77 K. This band is a plausible candidate for assignment as $^3[\pi \rightarrow \pi^*]$, based on its intensity and singlet–triplet splitting of 4500 cm^{-1}.

Che and co-workers have assigned the lowest energy absorption bands of a variety of $[Re(CAr)L_5]^+$ complexes as $^3[\pi \rightarrow \pi^*]$ (Table 2), on the basis of theoretical calculations [13]. Given this assignment, the singlet–triplet splittings for these compounds span the range 3500–8500 cm^{-1}. Although this has not been noted in the literature, the singlet–triplet splittings depend on aryl substituent and ancillary ligand in a manner that is difficult to rationalize and those at the upper end of the range are unexpectedly large. Also surprising are the high intensities (ε, 10^3) of some of the $^3[\pi \rightarrow \pi^*]$ bands. These observations may reflect strong mixing between the $^3[\pi \rightarrow \pi^*]$ state and other state(s); alternatively, the lowest energy absorption bands of some of the compounds may, in fact, arise from other electronic transitions. The $^3[\pi \rightarrow \pi^*]$ band has not been assigned for other metal–alkylidyne compounds.

2.3.2. $d_{xy} \rightarrow \pi^*$ and $\pi \rightarrow d_{xy}$ transitions and states

The characteristics of the $2a_2[d_{xy}] \rightarrow 3b_1[\pi^*(MCPh)]$ (d^1, d^2) and $2b_1[\pi(MCPh)] \rightarrow 2a_2[d_{xy}]$ (d^0, d^1) transitions of metal–alkylidyne compounds (Table 1; hereafter denoted $d_{xy} \rightarrow \pi^*$ and $\pi \rightarrow d_{xy}$, respectively) depend strongly on the ancillary ligands, aryl substituents, and particulars of spin–orbit coupling for the compound in question. Essentially all of the available experimental data are for d^2 complexes, so the following discussion focuses on their $d_{xy} \rightarrow \pi^*$ transitions.

For d^2 complexes $^1[d_{xy} \rightarrow \pi^*]$ and $^3[d_{xy} \rightarrow \pi^*]$ transitions are possible, although only the former have been reported. The $^1[d_{xy} \rightarrow \pi^*]$ band maxima for luminescent complexes are set out in Table 2. The band is typically relatively weak ($\varepsilon < 500$) despite the fact that the $^1[d_{xy} \rightarrow \pi^*]$ transition is both spin- and electric-dipole allowed; this is consistent with its formal d–d parentage (vide supra). The transition was first assigned by Bocarsly et al. [1,2] and McElwee-White and co-workers [3,4] for compounds of the types $W(CPh)(CO)_2L_2X$ (L = py, 1/2 tmeda, 1/2 dppe; X = Cl, Br, I) and $CpM(CPh)\{P(OMe)_3\}L$ (M = Mo, W; L = CO, $P(OMe)_3$) on the basis of molecular orbital calculations on model systems, which provided d_{xy} and π^* as the HOMO and LUMO, respectively. Experimental support for this assignment was provided by Manna et al. [27]. X-ray crystallographic studies of the d^2 compound $W(CPh)(dmpe)_2Br$ and its d^1 congener $[W(CPh)(dmpe)_2Br]^+$ revealed that their W≡C, W–Br, and W–P bond distances differ only slightly, as shown in Fig. 4, indicating that the redox orbital is essentially nonbonding; this is consistent with a d_{xy} HOMO. The lowest energy absorption band of the electronically similar complex $W(CPh)(PMe_3)_4Br$ exhibits a 1150 cm^{-1} vibronic progression at 77 K that arises from the WCPh oscillator (Fig. 4); although, it is not trivial to associate this frequency with a specific local mode, due to the fact that many of the WCPh

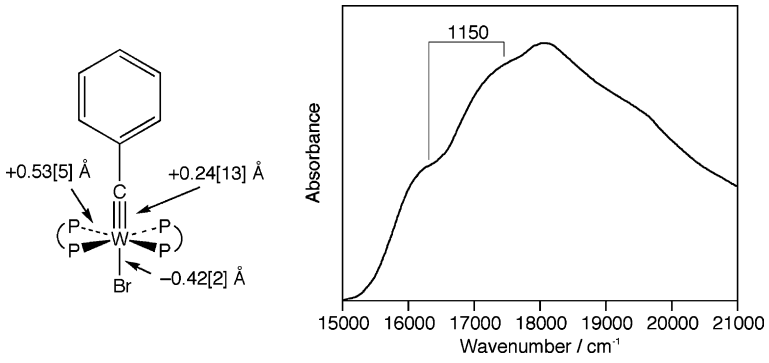

Fig. 4. Left: bond-distance changes of $W(CPh)(dmpe)_2Br$ upon one-electron oxidation; values in square brackets are the arithmetic mean of the estimated standard deviations of the bond distances in the two compounds. Right: $^1[d_{xy} \rightarrow \pi^*]$ electronic-absorption band of $W(CPh)(PMe_3)_4Br$ in 2-methylpentane at 77 K. Adapted from Ref. [27].

modes are of mixed W≡C and CPh character [22–24], the vibronic structure is indicative of an excited-state structural distortion within the WCPh fragment. Thus, the structural and spectroscopic data are fully consistent with the assignment of the lowest energy absorption band as $^1[d_{xy} \rightarrow \pi^*]$.

The $^1[d_{xy} \rightarrow \pi^*]$ transition energy of M(CPh)L_5 complexes is affected by the nature of the ancillary ligands. The equatorial ligands influence the transition energy principally via π interactions with the d_{xy} orbital (vide supra). This is nicely illustrated by the following series of W(CPh)L_4Cl compounds, for which the band red shifts with decreasing π-acceptor character of the equatorial ligands: W(CPh)$(CO)_2$(dppe)Cl, 435 nm; W(CPh)$(dppe)_2$Cl, 525 nm; W(CPh)$(depe)_2$Cl, 532 nm (Table 2). The axial ligand does not interact with the d_{xy} orbital, by symmetry, but can affect the energy of the M≡C π^* orbitals. For luminescent compounds (Table 2), the range of axial ligands employed is fairly narrow and so large effects have not been observed. For example, the $^1[d_{xy} \rightarrow \pi^*]$ band maximum shifts 300 cm^{-1} (448–454 nm) with halide substitution within the series of compounds W(CPh)$(CO)_2$(tmeda)X (X = Cl, Br, I) [1,2]. Larger band shifts have been observed for derivatives with unsaturated axial ligands, although emission from these compounds has not been observed. An example is provided by the series of compounds of type W(CH)$(dmpe)_2$(CCR), for which the $^1[d_{xy} \rightarrow \pi^*]$ band red shifts with extension of alkynyl R group π conjugation (R = H, 449 nm; $SiMe_3$, 458 nm; Ph, 470 nm; $C_6H_4CCBu^n$, 494 nm) [28].

There is a well developed theoretical framework for interpreting the $^1[d_{xy} \rightarrow \pi^*]$ and $^3[d_{xy} \rightarrow \pi^*]$ transition energies of tetragonally symmetric (D_{4h}, C_{4v}) metal–oxo and –nitrido complexes [19]. This treatment cannot be directly applied to M(CPh)L_5 compounds, however, because their lower symmetry (C_{2v}) introduces potential complexities with respect to the effects of spin–orbit coupling. We recently described [29] the theoretical implications for $^{1,3}[d_{xy} \rightarrow \pi^*]$ transitions of distortions from C_{4v} to C_{2v} symmetry in the course of interpreting the electronic spectra of d^2 ions of the type $[MoOL_4Cl]^+$ (L = PMe_3, 1/2 $Me_2PCH_2CH_2PMe_2$ (dmpe)); for these complexes, the C_{2v} symmetry is enforced by the phosphine ligands rather than by the multiply bonded ligand, but this difference is irrelevant with respect to the theoretical description of these states. What follows is an adaptation of that treatment to M(CPh)L_5 complexes.

Consider first the $d_{xy} \rightarrow \pi^*$ excited states of an idealized C_{4v} symmetry M(CH)L_5 complex (Fig. 1), which are strictly analogous to those of a ML_5 or NL_5 compound of identical symmetry [19]. The $^1[d_{xy} \rightarrow \pi^*]$ and $^3[d_{xy} \rightarrow \pi^*]$ transitions produce ^{1}E and ^{3}E excited states, respectively; these are separated in energy by the two-electron term $2K_{xy}$, where $K_{xy} = 3B + C$ for the $(t_{2g})^2$ configuration. Spin–orbit coupling splits the ^{3}E state into three sublevels (A_1,A_2(^{3}E), E(^{3}E), and B_1,B_2(^{3}E), in order of decreasing energy) that are dispersed in energy by ζ, the spin–orbit coupling constant. These levels are shown on the left-hand side of Fig. 5. The E(^{1}E) and E(^{3}E) spin–orbit states are mixed, with the extent of mixing depending on the magnitude of K_{xy} and ζ and being strongest for a third-row metal ion. One manifestation of this mixing is that the formally spin-forbidden $A_1(^1A_1) \rightarrow E(^3E)$ transition steals intensity from the spin-allowed $A_1(^1A_1) \rightarrow E(^1E)$ transition. This mixing is undoubtedly also of importance in determining the rate and efficiency of intersystem crossing, although there are no experimental measurements of these parameters for metal–alkylidyne complexes.

For a C_{2v} symmetry M(CPh)L_5 complex, the degeneracy of the π^* orbitals (and E states) is lifted. There are two $d_{xy} \rightarrow \pi^*$ transitions, $^{1,3}[d_{xy} \rightarrow \pi^*(MCPh)]$ ($2a_2 \rightarrow 3b_1$) and $^{1,3}[d_{xy} \rightarrow \pi^*(MC)]$ ($2a_2 \rightarrow 2b_2$, Fig. 2), which give rise to six spin–orbit levels. The extent of the interactions among these states is governed not only by K_{xy} and ζ, but also by the magnitude of π conjugation between the MC and Ph moieties (measured by the splitting, V, shown in Fig. 2) relative to these energies. Depicted on the right-hand side of Fig. 5 are the results of a ligand-field calculation that quantifies the energies of the $d_{xy} \rightarrow \pi^*$ excited states as a function of V, using a value of ζ appropriate for a third-row transition metal. The mixings among states are strongest near $V = 2K_{xy}$, at which there is an avoided crossing between B_2 spin–orbit states, but the picture progressively simplifies for $V > 2K_{xy}$. In the $V \gg 2K_{xy}$ limit, the $^1B_1/^3B_1$ [$d_{xy} \rightarrow \pi^*$(MC)] and $^1B_2/^3B_2$ [$d_{xy} \rightarrow \pi^*$(MCPh)] pairs of states derived from ^{1}E/^{3}E are well separated; mixing between like-symmetry spin–orbit states is small due to the large energy gaps between them [29].

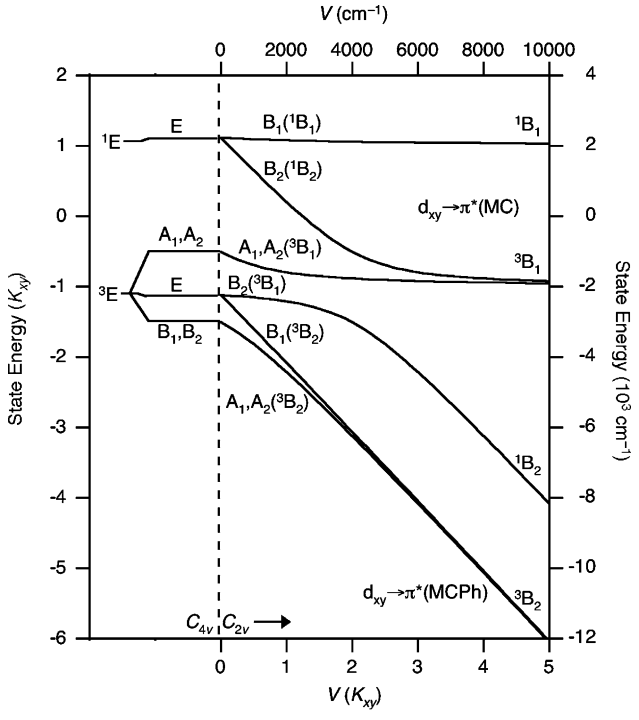

Fig. 5. Effects of spin–orbit coupling (ζ) and the splitting (V) of the π^*(MC) and π^*(MCPh) orbitals on the energies of the ^{1}E and ^{3}E parentage $d_{xy} \rightarrow \pi^*$ excited states ($2K_{xy} = 4000\ cm^{-1}$ and $\zeta = 2000\ cm^{-1}$). Left: C_{4v} symmetry and right: C_{2v} symmetry.

The electronic-absorption spectra of the C_{2v} symmetry $[MoOL_4Cl]^+$ ions indicate they reside near $V \cong 2K_{xy}$; their $d_{xy} \rightarrow \pi^*$ bands exhibit unusual energies and intensities as a result of the strong mixing among spin–orbit states in this region [29]. Metal–benzylidyne complexes, in contrast, appear to lie toward the limit $V \gg 2K_{xy}$. Experimentally, this is manifested by the fact that the $^1[d_{xy} \rightarrow \pi^*]$ bands of $M(CPh)L_5$ compounds are strongly red shifted from those of analogues with cylindrically symmetric alkylidyne R groups. For example, the $^1[d_{xy} \rightarrow \pi^*]$ band of $W(CPh)(depe)_2Cl$ ($\lambda_{max} = 532$ nm, Fig. 3) is red shifted 6000 cm^{-1} relative to that of $W(CH)(dmpe)_2Cl$ (403 nm [28,30]), while between $W(CPh)(CO)_2(tmeda)Cl$ and $W(CBu^t)(CO)_2(tmeda)Cl$ a red shift of 5200 cm^{-1} is observed [1,2]. Taking the compounds $W(CH)(dmpe)_2Cl$ and $W(CBu^t)(CO)_2(tmeda)Cl$ to represent the C_{4v} limit, these shifts are experimental measures of V at the level of approximation of Fig. 2. Theoretical calculations on $Cr(CPh)(CO)_4Cl$ [31] and $CpW(CPh)(CO)\{P(OMe)_3\}$ [4] suggest that V is even larger (>10,000 cm^{-1}). Consequently, mixing between the $^1[d_{xy} \rightarrow \pi^*]$ and $^3[d_{xy} \rightarrow \pi^*]$ states of $M(CPh)L_5$ complexes is anticipated to be small. One manifestation of this is that the $^3[d_{xy} \rightarrow \pi^*]$ band should be very weak due to the limited intensity stealing from $^1[d_{xy} \rightarrow \pi^*]$. Indeed, the $^3[d_{xy} \rightarrow \pi^*]$ band has not been observed for any metal–alkylidyne complex. Examination of the red flank of the $^1[d_{xy} \rightarrow \pi^*]$ band of $W(CPh)(depe)_2Cl$ (Fig. 3) shows only a featureless, Gaussian decay into the baseline in the region in which the $^3[d_{xy} \rightarrow \pi^*]$ band should be found.

The above treatment also applies to $^1[\pi \rightarrow d_{xy}]$ and $^3[\pi \rightarrow d_{xy}]$ excited states of d^0 $M(CPh)L_5$ complexes; from a symmetry standpoint, these are identical to the $d_{xy} \rightarrow \pi^*$ excited states of their d^2 analogues. To date, however, there have been no detailed spectroscopic studies of these chromophores (although d^0 $M(NAr)L_5$ metal–imido complexes have been described [32]). For d^1 complexes, both $^2[d_{xy} \rightarrow \pi^*]$ and $^2[\pi \rightarrow d_{xy}]$ transitions ($^2A_2 \rightarrow {}^2B_1$) are possible (Table 1). These bands should exhibit similar (weak) intensities and, thus, might be difficult to distinguish. Data have been reported for only two compounds [14], so detailed conclusions are not possible.

3. Photophysical properties of d^2 complexes

3.1. Emissive $d_{xy} \rightarrow \pi^*$ excited states

A variety of d^2 molybdenum– and tungsten–alkylidyne complexes luminesce in solution from what has been assigned as a $^3[d_{xy} \rightarrow \pi^*]$ excited state [1–8,10,11]. These compounds are of the general types **1**–**4** below. Electronic-spectroscopic and photophysical data for these complexes are set out in Table 2. At room temperature, luminescence lifetimes and quantum yields lie in the ranges $\tau = 10$–500 ns and $\phi = 10^{-4}$ to 10^{-2}, respectively. The assignment of the emissive state is based on the overlap of the emission band with the red tail of the $^1[d_{xy} \rightarrow \pi^*]$ absorption band; as noted above, the $^3[d_{xy} \rightarrow \pi^*]$ absorption band has not been observed. The spin-triplet character of the emissive state has been established through energy-transfer quenching studies of compounds of type **1** ($W(CPh)(CO)_2(py)_2Br$ [2]) and **4** ($CpW(CAr)(CO)\{P(OMe)_3\}$ [3]); these measurements place the energy of the state in the region of overlap between the absorption and emission bands. The very similar radiative rate constants observed for all derivatives of types **1**–**4** (ca. 10^3 s^{-1}, Table 2) strongly suggests that the emissive states of these species are also spin-triplets. At 77 K, the emission lifetimes of compounds of type **4** lengthen to several microseconds, which points strongly to the luminescent transition being spin-forbidden [4].

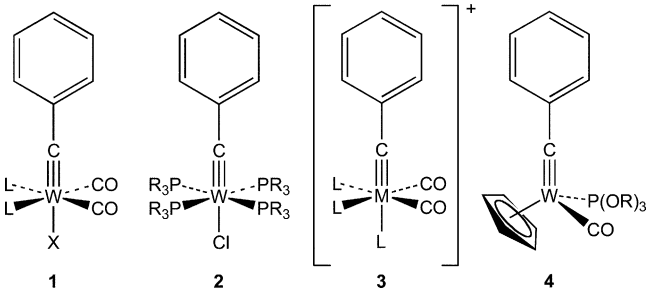

There is little quantitative information concerning the molecular structures of these compounds in their $^3[d_{xy} \rightarrow \pi^*]$ excited states. Vibronically structured emission spectra have not been observed; Franck–Condon analysis would be difficult, in any case, due to the complicated parentage of MCPh vibrational modes [22–24]. On simple molecular orbital grounds (Fig. 2), it is anticipated that the metal–carbon bond will be elongated in the excited state because the formal bond order is reduced from 3 to 2.5. There has also been speculation that the M≡C–Ph linkage will bend [2,3], based on a suggestion by Vogler et al. [33]. On the other hand, the absence of a significant difference in emission energy and band shape for compounds of type **4** between room temperature and 77 K has been interpreted as indicating that inner-sphere (and outer-sphere) reorganization in the excited state is small [4]. Recently, Chen probed the structure of the $^3[d_{xy} \rightarrow \pi^*]$ excited state for the compound $W(CPh)(dppe)_2Cl$ (**2**) through time-resolved XAFS measurements [34]. Although the question of WCPh bending could not be resolved, it was found that the W≡C bond is ca. 0.07 Å longer in the excited state than in the ground state. This distortion is similar in magnitude to that found for the related metal–oxo ions of the type $[MoOL_4Cl]^+$ for the $^1[d_{xy} \rightarrow \pi^*]$ excited state ($\Delta d(MoO) = 0.09$ Å) via Franck–Condon analysis of the vibronically structured absorption band [29]. It may not be reasonable to assume that this is a representative distortion for all emissive $W(CPh)L_5$ compounds, however, because $W(CPh)(dppe)_2Cl$ has the smallest Stokes' shift of any of these compounds (4200 cm^{-1}); other derivatives exhibit shifts of up to 8000 cm^{-1} (Table 2), indicative of larger excited-state distortions and/or singlet–triplet splittings.

The emissive $^3[d_{xy} \rightarrow \pi^*]$ has been probed by transient-absorption spectroscopy for CpM(CR)L(CO) (M = Mo, W) complexes of type **4** by Schanze and McElwee-White and co-workers [4,5]. For the tungsten complexes CpW(CPh){P(OMe)$_3$}(CO), CpW(CPh){P(OPh)$_3$}(CO), and CpW(C-2-Np){P(OMe)$_3$}(CO), which luminesce in solution, kinetic analysis of the transient spectra yields excited-state lifetimes in close agreement with the emission lifetimes, confirming that they correspond to the emissive state. These spectra, and that of the nonemissive molybdenum analogue CpMo(CPh){P(OMe)$_3$}(CO), exhibit very similar features, the dominant one being a strong absorption at 425–460 nm ($\Delta\varepsilon = 3000\ M^{-1}\ cm^{-1}$ for CpW(CPh){P(OMe)$_3$}(CO)) that is tentatively assigned to an allowed (triplet–triplet) $\pi \rightarrow \pi^*$ transition.

Despite the growing body of photophysical data for group 6 complexes, there has not been a detailed investigation of the nonradiative decay mechanisms of the emissive $^3[d_{xy} \rightarrow \pi^*]$ state. The W(CPh)L$_n$ compounds of types **1**–**4** do not collectively follow the energy-gap law; a plot (not shown) of ln (k_{nr}) versus E_T (approximated by $\bar{\nu}_{max}$) exhibits a high degree of scatter. Examination of the data (Table 2) reveals that variation of the metal, ancillary ligands, and alkylidyne R groups can all strongly affect the luminescence efficiency, suggesting that it may be difficult to pinpoint specific decay pathways. Generally speaking, neutral W(CPh)L$_5$ compounds (**1**,**2**) exhibit longer lifetimes and higher quantum yields than cationic derivatives (**3**) and the Cp derivatives (**4**), although the variations are not large for the most part. Other substitutions, though, lead to complete quenching of emission. It has been noted for both W(CPh)(CO)$_2$L$_2$Cl [1,2] and CpW(CPh)(CO){P(OMe)$_3$} [3] that replacement of the phenyl alkylidyne R group with an alkyl group leads to loss of emission. Replacement of tungsten with molybdenum in the compounds CpM(CPh)(CO){P(OMe)$_3$} (**4**) [4] and [(Me$_3$TACN)M(CPh)(CO)$_2$]$^+$ (**3**) [6] also leads to nonemissive compounds (although for [(η^3-Ppy$_3$)M(CPh)(CO)$_2$]$^+$ (**3**) both the molybdenum and tungsten compounds are luminescent [7]). Interestingly, for compounds of type **4**, only the mixed carbonyl/phosphite derivatives CpW(CPh)(CO){P(OR)$_3$} luminesce; the compounds CpW(CPh)(CO)$_2$ and CpW(CPh){P(OR)$_3$}$_2$ do not. Che and co-workers reported that while several derivatives [*fac*-LW(CPh)(CO)$_2$]$^+$ (**3**; L = Ppy$_3$, Me$_3$TACN) luminesce in solution, the TTCN derivative (TTCN: 1,4,7-trithiacyclononane) is not emissive [7]. Clearly, understanding the electronic origins of these effects will require additional study.

The emissive $^3[d_{xy} \rightarrow \pi^*]$ states of M(CPh)L$_5$ complexes can be quenched via bimolecular electron-transfer reactions that result in one-electron oxidation or reduction of the complex (Eqs. (1) and (2)). Bocarsly et al. reported that excited W(CPh)(CO)$_2$(tmeda) (**1**) is reductively quenched by *N*,*N*,*N*′,*N*′-tetramethyl-*p*-phenylenediamine and oxidatively quenched by *N*,*N*′-dimethyl-4,4′-bipyridinium [2]. These reactions are only partially reversible, as indicated by incomplete recovery of the ground state of the chromophore, suggesting that the 17-e$^-$ and 19-e$^-$ radical species that are generated undergo subsequent thermal reactions. Schanze and McElwee-White and co-workers carried out a detailed investigation of the oxidative quenching of the emissive state of CpW(CPh)(CO){P(OPh)$_3$} (**4**) with pyridinium and nitroaromatic acceptors [5]. Here too, the electron-transfer reactions are irreversible. An analysis of the data using Marcus theory allowed determination of the excited-state oxidation potential of the compound ($E(W^{IV*}/W^V) = -1.7$ V versus SCE) and indicated that the reorganization energy is relatively small ($\lambda < 0.40$ eV). Torraca and McElwee-White and have extensively studied the photochemical reactions of CpM(CR)L$_2$ compounds in halocarbon solution, in which excited-state electron transfer to the solvent initiates a rich thermal reaction chemistry. This work has been reviewed elsewhere [35].

$$[M(CPh)L_5]^* + A \rightarrow [M(CPh)L_5]^+ + A^- \quad (1)$$

$$[M(CPh)L_5]^* + D \rightarrow [M(CPh)L_5]^- + D^+ \quad (2)$$

In addition to the group 6 metal–alkylidyne derivatives, the d^2 ion [Os(CPh)(NH$_3$)$_5$]$^{3+}$ (**5**) also exhibits luminescence from a $^3[d_{xy} \rightarrow \pi^*]$ excited state [9]. The spin-triplet character of the emissive state was established by energy-transfer quenching. This chromophore is simple enough to allow the nonradiative decay pathways of the emissive state to be probed. Isotopic substitution of NH$_3$ ligands with ND$_3$ increases the emission lifetime and quantum yield, principally affecting k_{nr} (Table 2), thus implicating these ligands in the deactivation of the emissive state. Curiously, the quantum yield is wavelength dependent within the $^1[d_{xy} \rightarrow \pi^*]$ band envelope, complicating this interpretation. The emission is quenched by substituted pyridines; the quenching rate constant correlates with the pK_a of the pyridine and also exhibits a modest NH$_3$/ND$_3$ isotope effect, which is strongly suggestive of a proton-transfer quenching mechanism.

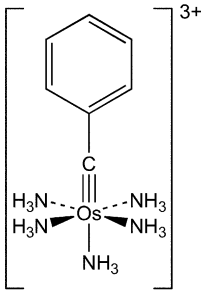

5

Emissive d^2 metal–alkylidyne complexes have also begun to be used as building blocks for materials in which the luminescence properties could impart electronic functionality. Mayr et al. described an interesting series of multimetallic complexes in which an isonitrile substituent incorporated onto the alkylidyne R group (**6**) allows assembly of extended structures (**7**) [10]. Relative to the parent W(CPh)(CO)$_2$L$_2$Cl compounds (**1**), the emission band of the monometallic compounds (**6**) red shifts as the conjuga-

tion is extended and, interestingly, the emission lifetimes increase, despite the smaller energy gap between ground and excited state. Coordination of these compounds to *cis*-$PdCl_2$, *cis*-PdI_2, *cis*-PtI_2, and *fac*-$ReCl(CO)_3$ fragments results in trimetallic complexes (**7**). All of these compounds except **7b** and **c** are luminescent; the emission bands are red shifted from those of the building blocks (**6**) and the emission lifetimes are slightly reduced. The emissive state was assigned as $^3[d_{xy} \rightarrow \pi^*]$ on the basis of the similar transition energies of **6** and **7** and the fact that model $ML_m(CNAr)_2$ compounds are not luminescent. The quenching of the emission in the PdX_2 derivatives **7b** and **c** was attributed to excited-state W → Pd electron transfer, which should be energetically favorable; energy-transfer quenching was excluded specifically for **7b** due to the absence of sufficiently low-lying excited states for the palladium fragment. The emission of the extended palladium compound **7f** is weaker than the other luminescent trimetallic complexes, suggesting that the emission of this compound may be only partially quenched by electron transfer.

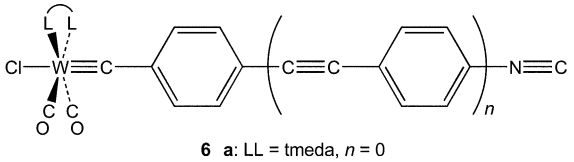

6 **a**: LL = tmeda, *n* = 0
b: LL = dppe, *n* = 0
c: LL = dppe, *n* = 1

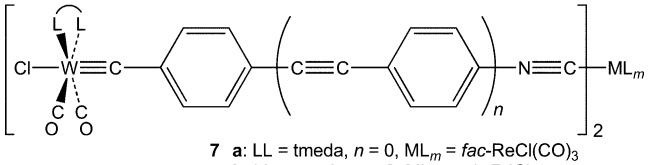

7 **a**: LL = tmeda, *n* = 0, ML_m = *fac*-$ReCl(CO)_3$
b: LL = tmeda, *n* = 0, ML_m = *cis*-$PdCl_2$
c: LL = tmeda, *n* = 0, ML_m = *cis*-PdI_2
d: LL = tmeda, *n* = 0, ML_m = *cis*-PtI_2
e: LL = dppe, *n* = 0, ML_m = *fac*-$ReCl(CO)_3$
f: LL = dppe, *n* = 1, ML_m = *cis*-PdI_2
g:LL = dppe, *n* = 1, ML_m = *cis*-PtI_2

Recently, Cohen et al. have investigated the tungsten–alkylidyne/zinc-porphyrin dyad **8** [11]. Preliminary evidence suggests that selective excitation into the porphyrin absorption bands in polar solvents initiates intramolecular electron transfer to rapidly produce a $[W]^+$–$[P_{Zn}]^-$ charge-separated species. In nonpolar solvent, the dyad exhibits unusual phosphorescence due to an equilibrium between the close lying $^3[d_{xy} \rightarrow \pi^*]$ and $^3[P_{Zn}]$ excited states.

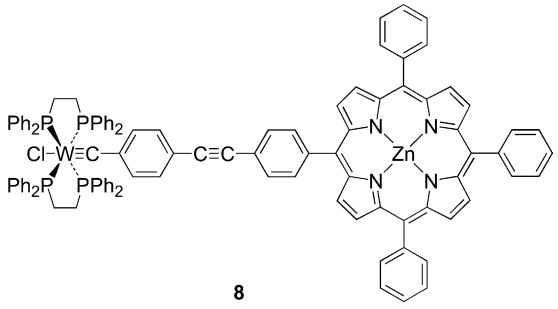

8

3.2. Emissive $\pi \rightarrow \pi^*$ excited states

In contrast to luminescent d^2 molybdenum and tungsten $M(CAr)L_5$ complexes, the analogous rhenium–alkylidyne compounds luminesce from an excited state assigned as $^3[\pi \rightarrow \pi^*]$ [12,13]. The compounds, of types **9**–**13** below, are diverse in composition, allowing the effects of both the ancillary ligands and alkylidyne R group on the excited-state energies and properties to be systematically probed; complexes **9**–**12** bear a common mesityl alkylidyne R group but different ancillary ligands, while **13** contains a constant set of ancillary ligands but different R group substituents. The emission was initially assigned as arising from a $^3[d_{xy} \rightarrow \pi^*]$ excited state [12]; however, subsequent HF-SCF calculations on the model compounds $[Re(CPh)(H_2PCHCHPH_2)_2Cl]^+$ (**9**), $[Re(CPh)(PH_3)_2(CO)(H_2O)Cl]^+$ (**11**), and $[Re(CPh)(H_2PCHCHPH_2)(CO)_2(OH)]^+$ (**13**) yielded a π(ReCAr) HOMO and π^*(ReCAr) LUMO, and a CI-singles calculations on the model for **9** provided $^3[\pi \rightarrow \pi^*]$ as the lowest energy excited state [13]. On this basis, the emissive state was assigned as $^3[\pi \rightarrow \pi^*]$.

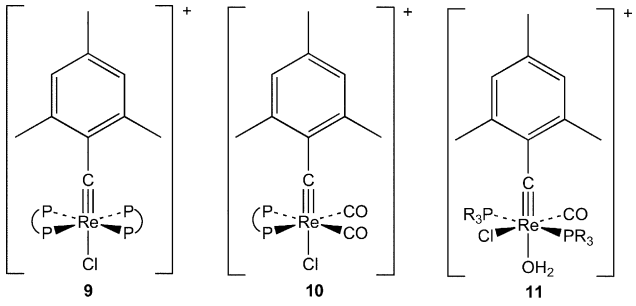

9 **10** **11**

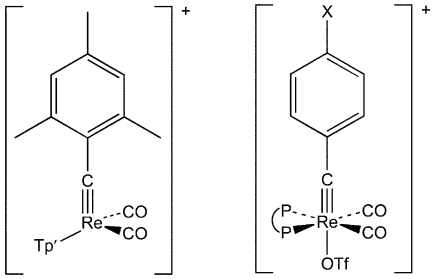

12 **13**

The emission spectra of the rhenium compounds exhibit several characteristics that point to the parentage of the emissive state being derived, at least in part, from ReCAr π symmetry orbitals. The emission bands of $[Re(CC_6H_4CN)(pdpp)(CO)_2(OTf)]^+$ (**13**), $[Re(CAr')(pdpp)_2Cl]^+$ (**9**), and $[Re(CAr')(PMePh_2)_2(CO)(H_2O)Cl]^+$ (**11**) exhibit vibronic structure at 77 K in the solid state and glassy solutions, consisting of a prominent 1100 cm^{-1} progression and hints of weaker, lower frequency features [12,13]. The 1100 cm^{-1} mode is certainly associated with the ReCAr moiety, indicating that there is a structural distortion within this fragment in the emissive excited state. In addition, for the $[Re(CC_6H_4X)(pdpp)(CO)_2(OTf)]^+$ derivatives of type **13** (X = H, Me, OMe, Cl, Br, CN), the emission band energy varies linearly with both the Hammett σ pa-

rameter of the aryl substituent X and the reduction potential associated with the alkylidyne R group [13]. These findings are consistent with the $^3[\pi \rightarrow \pi^*]$ assignment of the emissive state, but not uniquely so; they would also be consistent with an emissive $^3[d_{xy} \rightarrow \pi^*]$ excited state.

The emission lifetimes and quantum yields of these compounds vary by two orders of magnitude ($\tau = 20$ ns to 5 μs, $\phi = 10^{-4}$ to 10^{-2}); these are much broader ranges than seen for analogous group 6 complexes. Also in contrast to the group 6 complexes is the fact that the nonradiative-decay rates for the compounds $[Re(CAr')(pdpp)_2Cl]^+$ (**9**), $[Re(CAr')(PPh_3)_2(CO)(H_2O)Cl]^+$ (**11**), $[Re(CAr')(PMePh_2)_2(CO)(H_2O)Cl]^+$ (**11**), $[Re(CAr')\{P(C_6H_4OMe)_3\}_2(CO)(H_2O)Cl]^+$ (**11**), and $[Re(CAr')(dppe)(CO)_2Cl]^+$ (**10**) decrease with increasing excited-state energy according to the energy-gap law, suggesting that their excited-states share common deactivating mode(s) and have similar excited-state distortions.

The emissive excited states of rhenium–alkylidyne complexes can participate in electron-transfer reactions (Eqs. (1) and (2)) [12]. Both oxidative and reductive quenching has been demonstrated, though not in the same compound. The emission of the compound $[Re(CAr')(pdpp)_2Cl]^+$ (**9**) is oxidatively quenched by pyridinium acceptors; a Marcus analysis of the quenching rate constants provides $E(Re^{V*}/Re^{VI}) = -0.85$ V versus SCE. The compounds $[Re(CAr')(PPh_3)_2(CO)(H_2O)Cl]^+$ (**11**) and $[Re(CAr')(dppe)(CO)_2Cl]^+$ (**10**) undergo reductive quenching with various amine donors; a similar analysis provides $E(Re^{V*}/Re^{IV}) = +0.89$ and +0.88 V versus SCE, respectively. These excited-state potentials are consistent with estimates derived from the emission energies and ground-state electrode potentials of the complexes. Transient-absorption signals due to the oxidized donor and reduced acceptor were described as being long lived, suggesting that these are irreversible processes.

3.3. MLCT excited states

The d^2 $M(CAr)L_5$ complexes described above exhibit weak $^1[d_{xy} \rightarrow \pi^*]$ and $^3[\pi \rightarrow \pi^*]$ bands as the lowest energy features. If conjugated diimine ligands such as 1,10-phenanthroline or 2,2′-bipyridine are incorporated as ancillary ligands, however, an intense low-lying band assignable to a $^1[d \rightarrow \pi^*(diimine)]$ transition is observed and the photophysical properties of the compounds change significantly. Bocarsly et al. reported that the compound $W(CPh)(CO)_2(bpy)Cl$ does not luminesce and that $W(CPh)(CO)_2(phen)Cl$ exhibits an emission band whose position is sensitive to the polarity of the solvent [1,2]. These observations contrast with those for the related compound $W(CPh)(CO)_2(py)_2Cl$, which exhibits a solvent-insensitive emission band arising from the $^3[d_{xy} \rightarrow \pi^*]$ state. Che and co-workers have reported that the bipyridine derivatives $[Re(CAr')(bpy\text{-}X_2)(CO)_2Cl]^+$ (X = H, Cl, CO_2Me) exhibit an intense (ε, 10^4) band as the lowest lying absorption band [13]. The position of this band is strongly sensitive to the X substituent on the bipyridine ligand, decreasing in energy with increasing electron-withdrawing ability of X, consistent with assignment to a $^1[d \rightarrow \pi^*(bpy)]$ transition. These complexes also luminesce in fluid solution; the emissive state is tentatively ascribed to the MLCT excited state, although the shift of the emission band with X ($\Delta E = 800\ cm^{-1}$) is substantially less than that of the lowest absorption band ($\Delta E = 3800\ cm^{-1}$). The lifetimes and quantum yields of the emission (Table 2) are less than those of the related rhenium–phosphine derivatives (**10**), which luminesce from a $^3[\pi \rightarrow \pi^*]$ excited state.

4. Photophysical properties of d^1 complexes

Many d^2 octahedral metal–alkylidyne complexes undergo electrochemically reversible one-electron oxidations to d^1 congeners, several of which have been isolated and characterized. There is a single report, by Che and co-workers, of the photophysical properties of d^1 metal–alkylidyne compounds [14]. The octahedral complexes $Re(CAr')(PPh_3)(H_2O)X_3$ (**14**; Ar′ = 2,4,6-$Me_3C_6H_2$; X = Cl, Br) each exhibit two weak ($\varepsilon \sim 100$) electronic-absorption bands as the lowest energy features (Table 2). These bands were noted to have energies and intensities appropriate for $^2[d_{xy} \rightarrow \pi^*]$ transitions, as judged by comparison to emissive d^1 $MoOL_n$ ions [36]; only one of the two bands can be so assigned, however. Long-lived (ca. 400 ns) luminescence is observed from these compounds in dichloromethane solution, which was tentatively assigned to fluorescence from the $^2[d_{xy} \rightarrow \pi^*]$ excited state. The X → Re CT character of these transitions was inferred to be small due to the fact that the absorption and emission bands shift only slightly (<1000 cm^{-1}) as a function of X. The emissive state of $Re(CAr')(PPh_3)(H_2O)Cl_3$ is oxidatively quenched by *N*,*N*′-dimethyl-4,4′-bipyridinium.

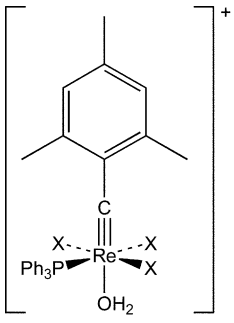

14

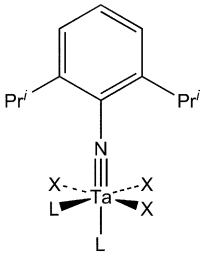

15

It is interesting to note the parallels between the photophysical and spectroscopic properties of these compounds and those of structurally related d^0 complexes of the type *cis*,*mer*-$M(NR)L_2X_3$ (**15**; M = Nb, Ta; R = 2,6-^{i}Pr$_2$-C_6H_3, *t*-Bu, adamantyl; L_2 = $MeOCH_2CH_2OMe$, tmeda, $(py)_2$, $(thf)_2$) studied by our group [32,37] and by Williams et al. [38]. The luminescent metal–arylimido derivatives exhibit a weak ($\varepsilon \sim 100$) absorption band between ca. 450–520 nm that is assigned to the $^1[\pi(M{\equiv}NAr) \rightarrow d_{xy}]$ transition [32]. The

shift of this band as a function of X is similar to that seen for the bands of the $Re(CAr')(PPh_3)(H_2O)X_3$ complexes; for the imido complexes, though, the $d_{xy} \rightarrow \pi^*(M{\equiv}NAr)$ assignment is precluded by the d^0 configuration. Given these similarities, it would appear that the assignment of the emissive state of the d^1 rhenium complexes as $^2[\pi(M{\equiv}CAr) \rightarrow d_{xy}]$ cannot be excluded; indeed, the observation of two weak absorption bands for the rhenium compounds could be an indication that the $^2[\pi(M{\equiv}CAr) \rightarrow d_{xy}]$ and $^2[d_{xy} \rightarrow \pi^*(M{\equiv}CAr)]$ states are close in energy.

5. Photophysical properties of d^0 complexes

The reaction chemistry of Schrock's $M(CR)(OR')_3$ complexes (M = Mo, W) has been extensively investigated due to their ability to catalyze alkyne-metathesis reactions [18]. The only study of the excited-state properties of these complexes was undertaken by Pollagi, who found that $W(CPh)(OBu^t)_3$ (**16**) exhibits strong, highly vibronically structured luminescence in the solid state at temperatures below 100 K but is not emissive in either the solid state or solution at room temperature [39].

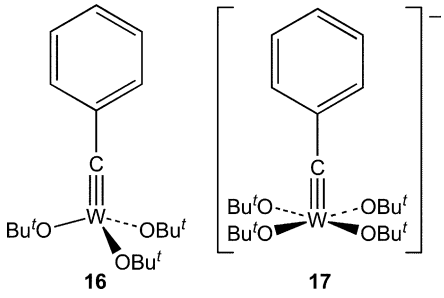

Addition of either a neutral or an anionic ligand to $W(CAr)(OBu^t)_3$ provides five-coordinate derivatives that luminesce in solution. Simpson discovered that $W(CPh)(OBu^t)_3$ reacts with the *t*-butoxide anion to give the square-pyramidal ion $[W(CPh)(OBu^t)_4]^-$ (**17**), which exhibits long-lived (μs) luminescence in solution at room temperature (Table 2) [15]. The long emission lifetime and extremely small radiative decay rate ($<10^2\ s^{-1}$) are consistent with the emissive state being of triplet spin-parentage. The electronic configuration of the emissive state could not be definitively assigned because the electronic-absorption spectrum does not display distinct features below the typical $\pi \rightarrow \pi^*$ absorption band in the UV region. Reference to Fig. 2 suggests that either $^3[\pi \rightarrow d_{xy}]$ or $^3[\pi \rightarrow \pi^*]$ states are logical candidates for the emissive state.

The spectroscopic and photophysical properties of the $[W(CPh)(OBu^t)_4]^-$ ion are cation and solvent dependent. X-ray crystallographic studies of the Na^+, $[Na(15\text{-crown-}5)]^+$, and $[Na(crypt\text{-}2,2,2)]^+$ salts of **17** indicate that the former two compounds possess strong Na–O interactions. In the solid state, the emission maxima of these salts range from ca. 600–700 nm and the lifetimes differ significantly from each other (Na**17**, 6.8 μs; [Na(15-crown-5)]**17**, 10.2 μs; [Na(crypt-2,2,2)]**17**, ∼300 ns). The lifetimes and emission maxima of the various salts of **17** are also observed to differ in solution (Table 2) and, furthermore, are solvent dependent; for example, the lifetime of [Na]**17** is 7.7 and 1.6 μs in 1,2-dimethoxyethane and acetonitrile solution, respectively. These observations suggest that Na–O interactions persist in organic solvents. Interestingly, these interactions enhance the photophysical properties of **17**; the emission lifetimes and quantum yield of [Na(crypt-2,2,2)]**17** are smaller than those of the salts compounds with more strongly coordinating cations.

The nonemissive $W(CR)(OBu^t)_3$ chromophore can also serve as a building block for coordination polymers that luminesce in the solid state and solution [16,40]. Pollagi et al. discovered that $W(C\text{–pyridyl})(OBu^t)_3$ compounds self-assemble to give solid materials composed of one-dimensional $[pyr\text{–}CW(OBu^t)_3]_\infty$ chains that are connected in a head-to-tail fashion via W–N bonds [16]. The coordination geometries of the polymers depend on the substitution pattern at the pyridyl ligand: the polymer composed of meta-substituted $W(C\text{–}3\text{-}C_5H_4N)(OBu^t)_3$ building blocks exhibits pseudo trigonal-bipyramidal coordination at tungsten ($[\mathbf{18}]_\infty$), whereas *para*-substituted $W(C\text{–}4\text{-}C_5H_2Me_2N)(OBu^t)_3$ forms a polymer in which the coordination at tungsten is pseudo square pyramidal ($[\mathbf{19}]_\infty$). The photophysical properties of the polymers in solution are complex, due to the fact that they dissolve to give a distribution of oligomers. In the solid state, they exhibit emission bands with similar maxima (∼640 nm). Although the emissive state has not been assigned, simple molecular orbital considerations suggest it almost certainly contains $\pi(W{\equiv}C\text{–pyr})$ and/or $\pi^*(W{\equiv}C\text{–pyr})$ orbital character; consistent with this, the emission band of $[\mathbf{19}]_\infty$ at 77 K exhibits a vibronic progression of ca. 1000 cm^{-1}, which arises from modes associated with the W≡C–pyr backbone.

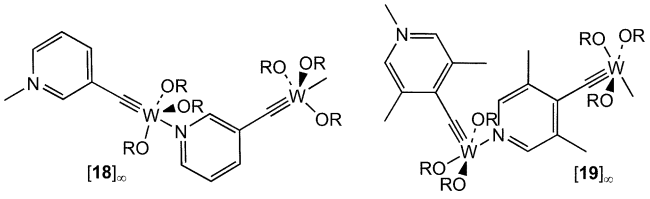

6. Concluding remarks

The variety of luminescent metal–alkylidyne complexes is striking: emission is observed from complexes with formal d^2, d^1, and d^0 electron counts, with ancillary ligands ranging from strong π acceptors to strong π donors, and from $d_{xy} \rightarrow \pi^*$, $\pi \rightarrow \pi^*$, $\pi \rightarrow d_{xy}$, and MLCT excited states. It seems likely that the present class of luminescent metal–alkylidyne complexes is just the tip of the iceberg, based on the fact that only a small fraction of known metal–alkylidyne complexes have been screened for emis-

sion. The rational design of compounds with particular luminescence properties will require a far more detailed understanding of the nonradiative decay pathways than is presently available; this is a challenge for future work. Such studies would be especially valuable to the development of metal–alkylidyne complexes as photoredox reagents and electronic materials.

Acknowledgments

This research was primarily supported by the NSF MRSEC Program under Grant DMR-0213745. We are grateful to Jibin Sun and Vivian Ferry for providing the data shown in Fig. 3.

References

[1] A.B. Bocarsly, R.E. Cameron, H.-D. Rubin, G.A. McDermott, C.R. Wolff, A. Mayr, Inorg. Chem. 24 (1985) 3976.
[2] A.B. Bocarsly, R.E. Cameron, A. Mayr, G.A. McDermott, in: H. Yersin, A. Vogler (Eds.), Photochemistry and Photophysics of Coordination Compounds, Springer-Verlag, Berlin, 1987, p. 213.
[3] J.D. Carter, K.B. Kingsbury, A. Wilde, T.K. Schoch, C.J. Leep, E.K. Pham, L. McElwee-White, J. Am. Chem. Soc. 113 (1991) 2947.
[4] T.K. Schoch, A.D. Main, R.D. Burton, L.A. Lucia, E.A. Robinson, K.S. Schanze, L. McElwee-White, Inorg. Chem. 35 (1996) 7769.
[5] C.C.S. Cavalheiro, K.E. Torraca, K.S. Schanze, L. McElwee-White, Inorg. Chem. 38 (1999) 3254.
[6] F.-W. Lee, M.C.-W. Chan, K.-K. Cheung, C.-M. Che, J. Organomet. Chem. 552 (1998) 255.
[7] F.-W. Lee, M.C.-W. Chan, K.-K. Cheung, C.-M. Che, J. Organomet. Chem. 563 (1998) 191.
[8] S.-W. Lai, M.C.-W. Chan, Y. Wang, H.-W. Lam, S.-M. Peng, C.-M. Che, J. Organomet. Chem. 617–618 (2001) 133.
[9] S. Trammell, B.P. Sullivan, L.M. Hodges, W.D. Harmon, S.R. Smith, H.H. Thorp, Inorg. Chem. 34 (1995) 2791.
[10] A. Mayr, M.P.Y. Yu, V.W.-W. Yam, J. Am. Chem. Soc. 121 (1999) 1760.
[11] B.W. Cohen, S.D. Cummings, R.F. Dallinger, M.D. Hopkins, in preparation.
[12] W.-M. Xue, Y. Wang, T.C.W. Mak, C.-M. Che, J. Chem. Soc. Dalton Trans. (1996) 2827.
[13] W.-M. Xue, Y. Wang, M.C.-W. Chan, Z.-M. Su, K.-K. Cheung, C.-M. Che, Organometallics 17 (1998) 1946.
[14] W.-M. Xue, M.C.-W. Chan, T.C.W. Mak, C.-M. Che, Inorg. Chem. 36 (1997) 6437.
[15] C.K. Simpson, R.E. Da Re, T.P. Pollagi, I.M. Steele, R.F. Dallinger, M.D. Hopkins, Inorg. Chim. Acta 345 (2003) 309.
[16] T.P. Pollagi, S.J. Geib, M.D. Hopkins, J. Am. Chem. Soc. 116 (1994) 6051.
[17] J.W. Herndon, Coord. Chem. Rev. 248 (2004) 3, and earlier reviews in the series cited therein.
[18] R.R. Schrock, Chem. Rev. 102 (2002) 145.
[19] V.M. Miskowski, H.B. Gray, M.D. Hopkins, Adv. Trans. Met. Coord. Chem. 1 (1996) 159.
[20] G. Frenking, N. Fröhlich, Chem. Rev. 100 (2000) 717.
[21] J. Sun, V.E. Ferry, unpublished results.
[22] J. Manna, R.J. Kuk, R.F. Dallinger, M.D. Hopkins, J. Am. Chem. Soc. 116 (1994) 9793.
[23] J. Manna, R.F. Dallinger, V.M. Miskowski, M.D. Hopkins, J. Phys. Chem. B 104 (2000) 10928.
[24] N.Q. Dao, J. Organomet. Chem. 684 (2003) 82, and references therein.
[25] G.W. King, S.P. So, J. Mol. Spectrosc. 37 (1971) 543.
[26] G.W. King, S.P. So, J. Mol. Spectrosc. 37 (1971) 535.
[27] J. Manna, T.M. Gilbert, R.F. Dallinger, S.J. Geib, M.D. Hopkins, J. Am. Chem. Soc. 114 (1992) 5870.
[28] J. Manna, S.J. Geib, M.D. Hopkins, J. Am. Chem. Soc. 114 (1992) 9199.
[29] R.E. Da Re, M.D. Hopkins, Inorg. Chem. 41 (2002) 6973.
[30] J. Manna, L.A. Mlinar, R.J. Kuk, R.F. Dallinger, S.J. Geib, M.D. Hopkins, in: F.R. Kreißl (Ed.), Transition Metal Carbyne Complexes, Kluwer Academic Publishers, Dordrecht, 1993, p. 75.
[31] N.M. Kostic, R.F. Fenske, Organometallics 1 (1982) 489.
[32] K.S. Heinselman, M.D. Hopkins, J. Am. Chem. Soc. 117 (1995) 12340.
[33] A. Vogler, J. Kisslinger, W.R. Roper, Z. Naturforsch. 38b (1983) 1506.
[34] L.X. Chen, B.W. Cohen, M.D. Hopkins, in preparation.
[35] K.E. Torraca, L. McElwee-White, Coord. Chem. Rev. 206–207 (2000) 469.
[36] A.K. Mohammed, A.W. Maverick, Inorg. Chem. 31 (1992) 4441.
[37] K.S. Heinselman, V.M. Miskowski, S.J. Geib, L.C. Wang, M.D. Hopkins, Inorg. Chem. 36 (1997) 5530.
[38] D.S. Williams, D.W. Thompson, A.V. Korolev, J. Am. Chem. Soc. 118 (1996) 6526.
[39] T.P. Pollagi, Ph.D. Thesis, University of Pittsburgh, Pittsburgh, PA, 1995.
[40] H.A. Brison, T.P. Pollagi, T.C. Stoner, S.J. Geib, M.D. Hopkins, Chem. Commun. (1997) 1263.